ORIGINAL PAPER

EFFECTS OF THERMAL RADIATION AND CHEMICAL REACTION ON UNSTEADY HYDROMAGNETIC MIXED CONVECTION FLOW PAST AN INFINITE VERTICAL PLATE

DEEPA GADIPALLY[1], MURALI GUNDAGANI[2], NARENDRA N.V. BABU[3]

Manuscript received: 07.03.2018; Accepted paper: 22.06.2018;
Published online: 30.09.2018.

Abstract. *In this research work, the combined effects of thermal radiation and chemical reaction on an unsteady hydromagnetic mixed convective flow of incompressible and electrically conducting fluids past an infinite vertical porous plate has been made in presence of Soret and Dufour numbers. Energy equation takes into account of viscous dissipation, thermal radiation and Dufour effects. The governing differential equations are transformed into a set of non – linear coupled ordinary differential equations and solved using similarity analysis with finite difference numerical technique using appropriate boundary conditions for various physical parameters. Numerical solutions have been derived for the effects of different physical flow parameters on the velocity, temperature and concentration fields, skin – friction, rate of heat and mass transfer are discussed through graphs and results are physically interpreted.*

Keywords: *thermal radiation, chemical reaction, Soret and Dufour numbers, MHD, mixed convection.*

1. INTRODUCTION

In recent years the combined heat and mass transfer by mixed convection in a fluid saturated porous medium has its own role in many engineering application problems such as nuclear reactor design, geothermal systems, petroleum engineering applications, evaporation at the surface of a water body, energy transfer in a wet cooling tower and the flow in a desert cooler. A comprehensive account of the available information in this field is provided in recent books by Ingham et al. [1] and Vafai [2]. Kassoy [3] studied the effect of variable viscosity on the onset of convection in porous medium. Please use the article's title as file_name in small caps. Cheng and Minkowyz [4] studied the effect of free convection about a vertical plate embedded in a porous medium with application to heat transfer from a dike.

Bejan and Khair [5] studied the buoyancy induced heat and mass transfer from a vertical plate embedded in a saturated porous medium. Lai and Kulacki [6] studied the coupled heat and mass transfer by natural convection from vertical surface in a porous medium. The same authors [7] also studied the effect of variable viscosity on convection heat transfer along a vertical surface in a saturated porous medium. Elbashbeshy [7] investigated the effect of steady free convection flow with variable viscosity and thermal diffusivity along a vertical plate. Yih [8] analyzed the coupled heat and mass transfer in mixed convection

[1] Chaitanya Bharathi Institute of Technology, Department of Mathematics, 500075 Telangana, India.
E-mail: deepa.gadipally@gmail.com.
[2] J. B. Institute of Engineering and Technology, Department of Mathematics, 500075 Telangana, India.
[3] Sanjivani College of Engineering, Department of Engineering Science, 423603 Maharashtra, India.

about a wedge for variable wall temperature and concentration. Kumari [9] analyzed the effect of variable viscosity on free and mixed convection boundary layer flow from a horizontal surface in a saturated porous medium. Postelnicu et al. [10] investigated the effect of variable viscosity on forced convection over a horizontal flat plate in a porous medium with internal heat generation. Seddeek [11, 12] studied the effects of chemical reaction, variable viscosity and thermal diffusivity on mixed convection heat and mass transfer through porous media. Mohamed E – Ali [13] studied the effect of variable viscosity on mixed convection along a vertical plate. Alam et al. [14] analyzed the study of the combined free – forced convection and mass transfer flow past a vertical porous plate in a porous medium with heat generation and thermal diffusion. Pantokratoras [15] analyzed the effect of variable viscosity with constant wall temperature. The unsteady mixed convective mass transfer flow of a viscous incompressible and electrically conducting fluid past an accelerated infinite vertical porous flat plate with suction in the presence of transverse magnetic field has been analyzed by Ramana Reddy et al. [16].

Soret, Dufour and thermal radiation effect on MHD flows arise in many areas of engineering and applied physics. The study of such flow has application in MHD generators, chemical engineering, nuclear reactors, geothermal energy, and reservoir engineering and astrophysical studies. In nature, the assumption of the pure fluid is rather impossible. The presence of foreign mass in the fluid plays an important role in flow of fluid. Thermal diffusion or Soret effect is one of the mechanisms in the transport phenomena in which molecules are transported in a multi component mixture driven by temperature gradient. The inverse phenomena of thermal diffusion, if multi component mixture were initially at the same temperature, are allowed to diffuse into each other, there arises a difference of temperature in the system. Sparrow and Cess [17] analyzed the effect of magnetic field on free convection heat transfer. Alam et al. [18] investigated Dufour effect and Soret effect on MHD free convective heat and mass transfer flow past a vertical flat plate embedded in porous medium. Dursunkaya et al. [19] studied Diffusion thermo and thermal diffusion effect in transient and steady natural convection from vertical surface, Postelnicu [20] analyzed the influence of a magnetic field on heat and mass transfer by natural convection from vertical surface in porous media considering Soret and Dufour effects. Raptis et al. [21] discussed radiation and free convection flow past a moving plate. Satyanarayana [22] discussed the viscous dissipation and thermal radiation effects on an unsteady MHD convection flow past a semi - infinite vertical permeable moving porous plate. Alabraba et al. [23] investigated the interaction of mixed convection with thermal radiation in laminar boundary flow taking into account the binary chemical reaction and Soret and Dufour effects. Karim et al. [24] investigated Dufour and Soret effect on steady MHD flow in presence of heat generation and magnetic field past an inclined stretching sheet. Bhavana et al. [25] analyzed the Soret effect on free convective unsteady MHD flow over a vertical plate with heat source.

Motivated by the above reference work and the numerous possible industrial applications of the problem (like in isotope separation), it is of paramount interest in this study to investigate the effects thermal radiation, chemical reaction, Soret and Dufour on MHD flow along an accelerated infinite vertical porous flat plate. Hence, the purpose of this paper is to study the more general problem which includes the thermal radiation, chemical reaction, Soret and Dufour effects on an unsteady magnetohydrodynamic flow and heat transfer along an accelerated infinite vertical porous flat plate with mass transfer in presence of viscous dissipation. In this study, the effects of different flow parameters encountered in the equations are also studied. The problem is solved numerically using the finite difference scheme, which is more economical from the computational view point. The momentum, thermal, and solutal boundary layer equations are transformed into a set of ordinary differential equations and then solved using MATALAB bvp4c. The analysis of the results

obtained in the present work shows that the flow field is appreciably influenced by Dufour and Soret numbers, thermal radiation parameter and chemical reaction parameter on the wall. To reveal the tendency of the solutions, selected results for the velocity components, temperature, and concentration are graphically depicted. The rest of the paper is structured as follows. In Section 2, we formulate the problem, in Section 3, we give the method of solution. Our results are presented and discussed in Section 4 and in Section 5, we present some brief conclusions.

2. MATHEMATICAL FORMULATION

Consider the unsteady mixed convection mass transfer chemically reacting and thermal radiating flow of a viscous incompressible electrically conducting fluid past an accelerating vertical infinite porous flat plate with Soret and Dufour numbers. In Cartesian coordinate system, let axis is taken to be along the plate and the axis normal to the plate. Since the plate is considered infinite in direction, hence all physical quantities will be independent of direction. The wall is maintained at constant temperature and concentration higher than the ambient temperature and concentration respectively. A uniform magnetic field of magnitude is applied normal to the plate. The transverse applied magnetic field and magnetic Reynold's number are assumed to be very small, so that the induced magnetic field is negligible. It is assumed that there is no applied voltage which implies the absence of an electric field. It is assumed that the plate is accelerating with a velocity in its own plane for . The fluid has constant kinematic viscosity and constant thermal conductivity and the Boussinesq's approximation have been adopted for the flow. The magnetohydrodynamic unsteady mixed convective boundary layer equations under the Boussinesq's approximations are:

Continuity Equation:

$$\frac{\partial v'}{\partial y'} = 0 \Rightarrow v' = -v'_o \text{ (Constant)} \tag{1}$$

Momentum Equation:

$$\frac{\partial u'}{\partial t'} + v'\frac{\partial u'}{\partial y'} = g\beta\left(T' - T'_\infty\right) - \nu\frac{u'}{k'} + g\beta^*\left(C' - C'_\infty\right) + \nu\frac{\partial^2 u'}{\partial y'^2} - \frac{\sigma B_o^2}{\rho}u' \tag{2}$$

Energy Equation:

$$\frac{\partial T'}{\partial t'} + v'\frac{\partial T'}{\partial y'} = \frac{\kappa}{\rho\, c_p}\frac{\partial^2 T'}{\partial y'^2} + \frac{\nu}{c_p}\left(\frac{\partial u'}{\partial y'}\right)^2 + \frac{D_m k_T}{c_S c_P}\frac{\partial^2 C'}{\partial y'^2} - \frac{\partial q_r}{\partial y'} \tag{3}$$

Concentration Equation:

$$\frac{\partial C'}{\partial t'} + v'\frac{\partial C'}{\partial y'} = D\frac{\partial^2 C'}{\partial y'^2} + \frac{D_m k_T}{T_m}\frac{\partial^2 T'}{\partial y'^2} - K_r\left(C' - C'_\infty\right) \tag{4}$$

The boundary conditions of the problem are:

$$\left.\begin{aligned} t' \le 0 &: \{\, u' = 0,\ v' = 0,\ T' = 0,\ C' = 0 \ \ for\ all\ \ y' \\ t' > 0 &: \begin{cases} u' = U_O,\ v' = -v_o',\ T' = T_w',\ C' = C_w' \ \ at\ \ y' = 0 \\ u' \to 0,\ T' \to T_\infty',\ C' \to C_\infty' \ \ as\ \ y' \to \infty \end{cases} \end{aligned}\right\} \tag{5}$$

The radiative heat flux term is simplified by making use of the Rosseland approximation [26] as

$$q_r = -\frac{4\bar{\sigma}}{3k^*}\frac{\partial T'^4}{\partial y'} \tag{6}$$

Here $\bar{\sigma}$ is Stefan – Boltzmann constant and k^* is the mean absorption coefficient. It is assumed that the temperature differences within the flow are sufficiently small so that T'^4 can be expressed as a linear function of T' after using Taylor's series to expand T'^4 about the free stream temperature T_h' and neglecting higher – order terms. This results in the following approximation:

$$T'^4 \cong 4T_h'^3 T' - 3T_h'^4 \tag{7}$$

Using equations (6) and (7) in the last term of equation (2), we obtain:

$$\frac{\partial q_r}{\partial y'} = -\frac{16\bar{\sigma}T_h'^3}{3k^*}\frac{\partial^2 T'}{\partial y'^2} \tag{8}$$

Introducing (8) in the equation (2), the energy equation becomes:

$$\frac{\partial T'}{\partial t'} + v'\frac{\partial T'}{\partial y'} = \frac{\kappa}{\rho\, c_p}\frac{\partial^2 T'}{\partial y'^2} + \frac{\nu}{c_p}\left(\frac{\partial u'}{\partial y'}\right)^2 + \frac{D_m k_T}{c_S c_P}\frac{\partial^2 C'}{\partial y'^2} + \frac{16\bar{\sigma}T_h'^3}{3k^*}\frac{\partial^2 T'}{\partial y'^2} \tag{9}$$

Introducing the following non – dimensional variables and parameters,

$$\left.\begin{aligned} &y = \frac{y'v_o'}{\nu},\ t = \frac{t'v_o'^2}{4\nu},\ u = \frac{u'}{U_o},\ M = \left(\frac{\sigma B_o^2}{\rho}\right)\frac{\nu}{v_o'^2},\ K = \frac{k'\,v_o'^2}{\nu^2},\ Sc = \frac{\nu}{D},\ \mathrm{Pr} = \frac{\nu}{k}, \\ &\theta = \frac{T' - T_\infty'}{T_w' - T_\infty'},\ C = \frac{C' - C_\infty'}{C_w' - C_\infty'},\ Gr = \frac{\nu g\beta(T_w' - T_\infty')}{U_o v_o'^3},\ Gc = \frac{g\beta^*\nu(C_w' - C_\infty')}{U_o v_o'^3},\ R = \frac{\kappa k^*}{4\sigma T_h'^3}, \\ &Ec = \frac{v_o'^2}{c_p(T_w' - T_\infty')},\ Du = \frac{D_m k_T(C_w' - C_\infty')}{c_S c_P(T_w' - T_\infty')},\ Sr = \frac{D_m k_T(T_w' - T_\infty')}{\nu T_m(C_w' - C_\infty')},\ k_r = \frac{K_r\nu}{U_o^2} \end{aligned}\right\} \tag{10}$$

Substituting (10) in equations (2), (3) and (9) under boundary conditions (5), we get:

$$\frac{\partial u}{\partial t} - \frac{\partial u}{\partial y} = (Gr)\theta + (Gc)C + \frac{\partial^2 u}{\partial y^2} - \left(M + \frac{1}{K}\right)u \tag{11}$$

$$\frac{\partial \theta}{\partial t}-\frac{\partial \theta}{\partial y}=\frac{1}{\Pr}\left(\frac{3R+4}{3R}\right)\frac{\partial^2 \theta}{\partial y^2}+(Ec)\left(\frac{\partial u}{\partial y}\right)^2+Du\left(\frac{\partial^2 C}{\partial y^2}\right) \tag{12}$$

$$\frac{\partial C}{\partial t}-\frac{\partial C}{\partial y}=\frac{1}{Sc}\frac{\partial^2 C}{\partial y^2}+Sr\left(\frac{\partial^2 \theta}{\partial y^2}\right)-(k_r)C \tag{13}$$

The corresponding boundary conditions are:

$$\left.\begin{array}{l} t\le 0:\ \ u=0,\ \theta=0,\ C=0\ \ for\ all\ \ y \\ t>0:\ \begin{cases} u=1,\ \theta=1,\ C=1\ at\ \ y=0 \\ u\to 0,\ \theta\to 0,\ C\to 0\ \ as\ \ y\to\infty \end{cases} \end{array}\right\} \tag{14}$$

The skin – friction, Nusselt number and Sherwood number are important physical parameters for this type of boundary layer flow. The skin – friction at the plate, which in the non – dimensional form is given by

$$\tau=\frac{\tau'_w}{\rho U_o \nu}=\left(\frac{\partial u}{\partial y}\right)_{y=0} \tag{15}$$

The rate of heat transfer coefficient, which in the non – dimensional form in terms of the Nusselt number is given by

$$Nu=-x\frac{\left(\frac{\partial T'}{\partial y'}\right)_{y'=0}}{T'_w-T'_\infty}\ \ \Rightarrow Nu\,\mathrm{Re}_x^{-1}=-\left(\frac{\partial \theta}{\partial y}\right)_{y=0} \tag{16}$$

The rate of mass transfer coefficient, which in the non – dimensional form in terms of the Sherwood number, is given by

$$Sh=-x\frac{\left(\frac{\partial C'}{\partial y'}\right)_{y'=0}}{C'_w-C'_\infty}\ \ \Rightarrow Sh\,\mathrm{Re}_x^{-1}=-\left(\frac{\partial C}{\partial y}\right)_{y=0} \tag{17}$$

where $\mathrm{Re}=\frac{U_o x}{\nu}$ is the local Reynolds number.

3. METHOD OF SOLUTION

We shall solve the system of partial differential equations numerically using the finite difference technique and equations (11) – (13) yield:

$$\left(\frac{u_i^{j+1}-u_i^j}{\Delta t}\right)-\left(\frac{u_{i+1}^j-u_i^j}{\Delta y}\right)=\left(\frac{u_{i+1}^j-2u_i^j+u_{i-1}^j}{(\Delta y)^2}\right)-\left(M+\frac{1}{K}\right)u_i^j+(Gr)\theta_i^j+(Gc)C_i^j \tag{18}$$

$$\left(\frac{\theta_i^{j+1}-\theta_i^j}{\Delta t}\right)-\left(\frac{\theta_{i+1}^j-\theta_i^j}{\Delta y}\right)=\frac{1}{\Pr}\left(\frac{3R+4}{3R}\right)\left(\frac{\theta_{i+1}^j-2\theta_i^j+\theta_{i-1}^j}{(\Delta y)^2}\right)+(Ec)\left(\frac{u_{i+1}^j-u_i^j}{\Delta y}\right)^2+(Du)\left(\frac{C_{i+1}^j-2C_i^j+C_{i-1}^j}{(\Delta y)^2}\right) \tag{19}$$

$$\left(\frac{C_i^{j+1}-C_i^j}{\Delta t}\right)-\left(\frac{C_{i+1}^j-C_i^j}{\Delta y}\right)=\frac{1}{Sc}\left(\frac{C_{i+1}^j-2C_i^j+C_{i-1}^j}{(\Delta y)^2}\right)-(k_r)C_i^j+(Sr)\left(\frac{\theta_{i+1}^j-2\theta_i^j+\theta_{i-1}^j}{(\Delta y)^2}\right) \tag{20}$$

where the indices i and j refer to y and t respectively. The initial and boundary conditions (14) yield.

$$\begin{aligned} &t\le 0:\ \{u_i^j=0,\ \theta_i^j=0,\ C_i^j=0 \quad for\ all\ y \\ &t>0:\begin{cases} u_i^j=1,\ \theta_i^j=1,\ C_i^j=1\ at\ y=0 \\ u_i^j\to 0,\ \theta_i^j\to 0,\ C_i^j\to 0\ as\ y\to\infty \end{cases} \end{aligned} \tag{21}$$

The term consistency applied to a finite difference procedure means that the procedure may in fact approximate the solution of the partial differential equation under study and not the solution of any other partial differential equation. The consistency is measured in terms of the difference between a differential equation and a difference equation.

Here, we can write

$$\frac{\partial u}{\partial t}=\frac{u_i^{j+1}-u_i^j}{\Delta t}+O(\Delta t),\ \frac{\partial \theta}{\partial t}=\frac{\theta_i^{j+1}-\theta_i^j}{\Delta t}+O(\Delta t),\ \frac{\partial C}{\partial t}=\frac{C_i^{j+1}-C_i^j}{\Delta t}+O(\Delta t),$$

$$\frac{\partial u}{\partial y}=\frac{u_{i+1}^j-u_i^j}{\Delta y}+O(\Delta y),$$

$$\frac{\partial \theta}{\partial y}=\frac{\theta_{i+1}^j-\theta_i^j}{\Delta y}+O(\Delta y),\ \frac{\partial C}{\partial y}=\frac{C_{i+1}^j-C_i^j}{\Delta y}+O(\Delta y),\ \frac{\partial^2 u}{\partial y^2}=\frac{u_{i+1}^j-2u_i^j+u_{i-1}^j}{(\Delta y)^2}+O(\Delta y)^2,$$

$$\frac{\partial^2 \theta}{\partial y^2}=\frac{\theta_{i+1}^j-2\theta_i^j+\theta_{i-1}^j}{(\Delta y)^2}+O(\Delta y)^2 \text{ and } \frac{\partial^2 C}{\partial y^2}=\frac{C_{i+1}^j-2C_i^j+C_{i-1}^j}{(\Delta y)^2}+O(\Delta y)^2$$

For consistency of equation (18), we estimate

$$\begin{aligned} &\left\{\left(\frac{u_i^{j+1}-u_i^j}{\Delta t}\right)-\left(\frac{u_{i+1}^j-u_i^j}{\Delta y}\right)-\left(\frac{u_{i+1}^j-2u_i^j+u_{i-1}^j}{(\Delta y)^2}\right)+\left(M+\frac{1}{K}\right)u_i^j-(Gr)\theta_i^j-(Gc)C_i^j\right\} \\ &-\left\{\frac{\partial u}{\partial t}-\frac{\partial u}{\partial y}-(Gr)\theta-(Gc)C-\frac{\partial^2 u}{\partial y^2}+\left(M+\frac{1}{K}\right)u\right\}_{i,\,j}=O(\Delta t)+O(\Delta y) \end{aligned} \tag{22}$$

For consistency of equation (19), we estimate

$$\left\{\left(\frac{\theta_i^{j+1}-\theta_i^j}{\Delta t}\right)-\left(\frac{\theta_{i+1}^j-\theta_i^j}{\Delta y}\right)-\frac{1}{\Pr}\left(\frac{3R+4}{3R}\right)\left(\frac{\theta_{i+1}^j-2\theta_i^j+\theta_{i-1}^j}{(\Delta y)^2}\right)-(Ec)\left(\frac{u_{i+1}^j-u_i^j}{\Delta y}\right)^2-(Du)\left(\frac{C_{i+1}^j-2C_i^j+C_{i-1}^j}{(\Delta y)^2}\right)\right\}$$
$$-\left\{\frac{\partial\theta}{\partial t}-\frac{\partial\theta}{\partial y}-\frac{1}{\Pr}\left(\frac{3R+4}{3R}\right)\frac{\partial^2\theta}{\partial y^2}-(Ec)\left(\frac{\partial u}{\partial y}\right)^2-Du\left(\frac{\partial^2 C}{\partial y^2}\right)\right\}_{i,\,j}=O(\Delta t)+O(\Delta y) \tag{23}$$

Similarly with respect to equation (20)

$$\left\{\left(\frac{C_i^{j+1}-C_i^j}{\Delta t}\right)-\left(\frac{C_{i+1}^j-C_i^j}{\Delta y}\right)-\frac{1}{Sc}\left(\frac{C_{i+1}^j-2C_i^j+C_{i-1}^j}{(\Delta y)^2}\right)+(k_r)C_i^j-(Sr)\left(\frac{\theta_{i+1}^j-2\theta_i^j+\theta_{i-1}^j}{(\Delta y)^2}\right)\right\}$$
$$-\left\{\frac{\partial C}{\partial t}-\frac{\partial C}{\partial y}-\frac{1}{Sc}\frac{\partial^2 C}{\partial y^2}+(k_r)C-(Sr)\left(\frac{\partial^2\theta}{\partial y^2}\right)\right\}_{i,\,j}=O(\Delta t)+O(\Delta y) \tag{24}$$

Here, the right hand side of equations (22) – (24) represents truncation error as $\Delta t\to 0$ with $\Delta y\to 0$, the truncation error tends to zero. Hence our explicit scheme is consistent. Here Δy, Δt are mesh sizes along y and time direction respectively. The infinity taken as $i=1$ to n and the equations (22), (23) and (24) are solved under the boundary conditions (21), following the tri diagonal system of equations are obtained.

$$A_i X_i = B_i \ (i=1 \text{ to } n) \tag{25}$$

where A_i is the tri diagonal matrix of order $n\times n$ and X_i, B_i are the column matrices having n components. The above system of equations has been solved by Thomas Algorithm (Gauss elimination method), for velocity, temperature and concentration. In order to prove the convergence of the finite difference scheme, the computations are carried out for different values of Δt. But the Crank – Nicholson method is unconditionally stable. By changing the value of Δt there is no change in the study state condition. So, the finite difference scheme is convergent and stable.

4. RESULTS AND DISCUSSION

The profiles of velocity, temperature and concentration are shown in the figures from (1) to (14) respectively. The effect of the Hartmann number (M) is shown in Fig. 1. It is observed that the velocity of the fluid decreases with the increase of the magnetic field number values. The decrease in the velocity as the Hartmann number (M) increases is because the presence of a magnetic field in an electrically conducting fluid introduces a force called the Lorentz force, which acts against the flow if the magnetic field is applied in the normal direction, as in the present study. This resistive force slows down the fluid velocity component as shown in figure (1). The effect of Permeability parameter (K) is presented in the Fig. 2. From this figure we observe that, the velocity is increases with increasing values of K.

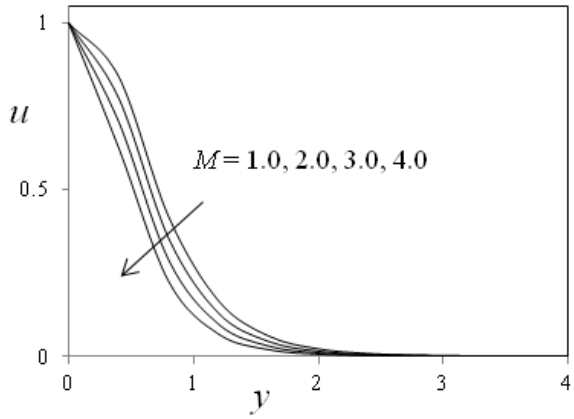

Figure 1. Velocity profiles for different values of *M*.

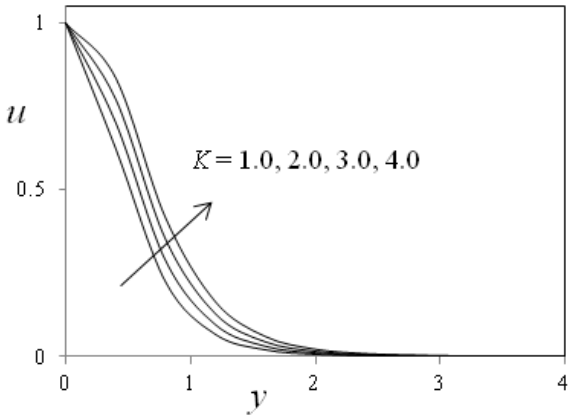

Figure 2. Velocity profiles for different values of *K*.

Figs. 3-4 illustrate the variation of velocity and temperature function for various values of the thermal radiation parameter (R). It is immediately apparent that velocity as well as temperature clearly increase as R rises from 1 to 3. Velocity reaches a maximum in close proximity to the wall and then falls gradually to zero at the edge of the boundary layer. Inspection of Fig. 4 shows that for a small value of R ($R<2$) temperature profile continuously decreases from the wall, while for higher values of R it increases attaining a maximum near the plate boundary and then decreases. As such there is a noticeable temperature overshoot with $R>1$ since considerable thermal energy is imparted via the presence of a thermal radiation source to the fluid causing an elevation in temperatures near the wall.

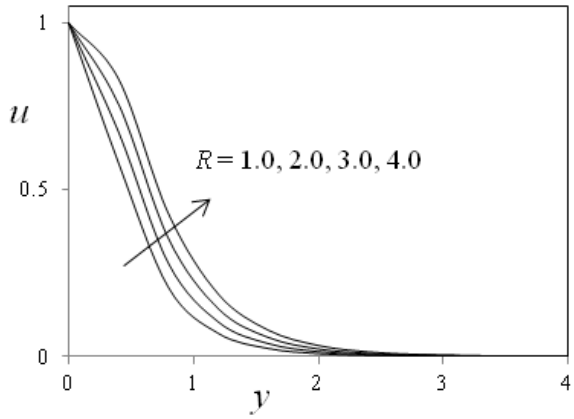

Figure 3. Velocity profiles for different values of *R*.

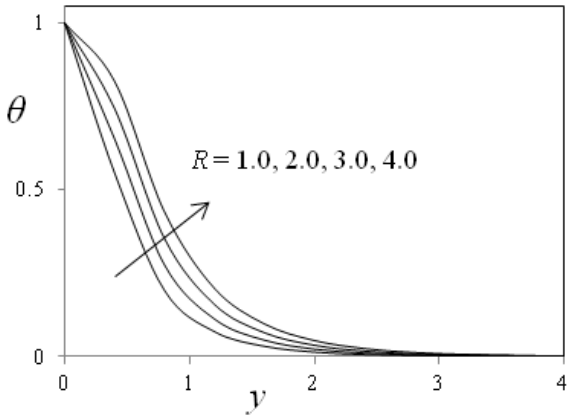

Figure 4. Temperature profiles for different values of *R*.

The influence of the viscous dissipation parameter i.e., the Eckert number (Ec) on the velocity and temperature are shown in Figs. 5-6. The Eckert number (Ec) expresses the relationship between the kinetic energy in the flow and the enthalpy. It embodies the conversion of kinetic energy into internal energy by work done against the viscous fluid stresses. Greater viscous dissipative heat causes a rise in the temperature as well as the velocity. This behavior is evident from Figs. 5-6.

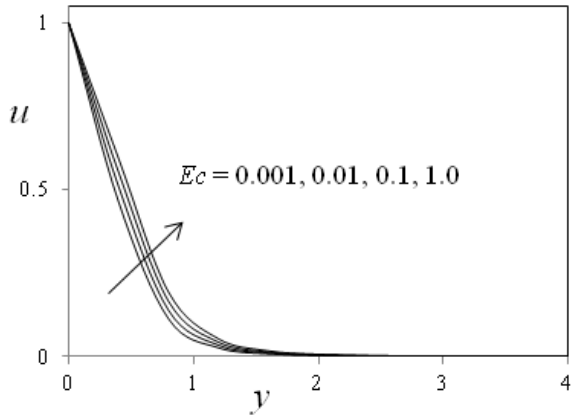

Figure 5. Velocity profiles for different values of *Ec*.

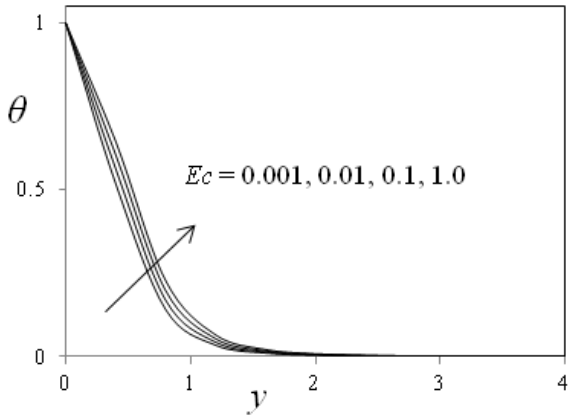

Figure 6. Temperature profiles for different values of *Ec*.

The variations of velocity distribution with y for different values of the Dufour number (Du) are shown in Fig. 7. In this figure, it can be clearly seen that as the Dufour number increases, the velocity increases. The variations of velocity distribution with y for different values of the Soret number (Sr) are shown in Fig. 8. It can be clearly seen that the velocity distribution in the boundary layer increases with the Soret number. It is interesting note that the effect of Dufour and Soret numbers on velocity field are little significant. This is because either a decrease in concentration difference or an increase in temperature difference leads to an increase in the value of the Soret parameter (Sr). Hence increasing the Soret parameter (Sr) increases the velocity of the fluid.

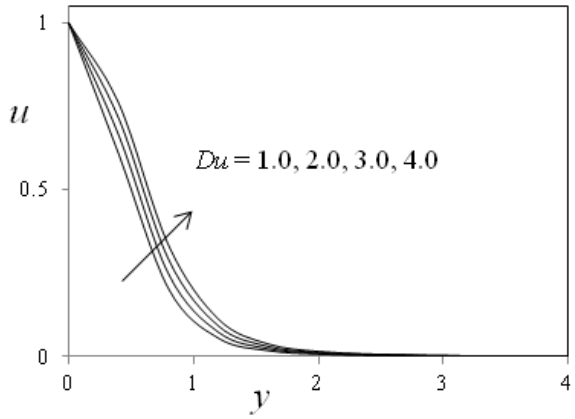

Figure 7. Velocity profiles for different values of *Du*.

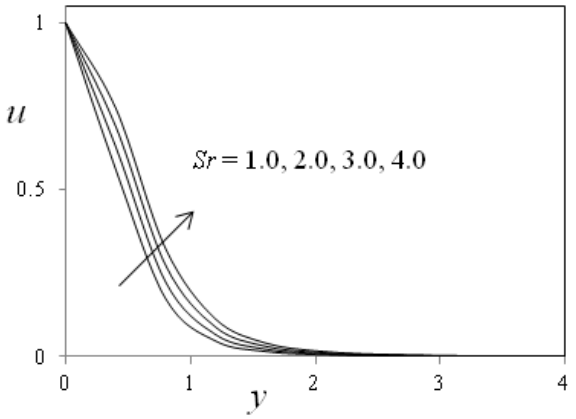

Figure 8. Velocity profiles for different values of *Sr*.

Figs. 9-10 display the effects of the chemical reaction parameter (k_r) on the velocity and concentration profiles, respectively. As expected, the presence of the chemical reaction significantly affects the concentration profiles as well as the velocity profiles. It should be mentioned that the studied case is for a destructive chemical reaction (k_r). In fact, as chemical reaction (k_r) increases, the considerable reduction in the velocity profiles is predicted, and the presence of the peak indicates that the maximum value of the velocity occurs in the body of the fluid close to the surface but not at the surface. Also, with an increase in the chemical reaction parameter, the concentration decreases. It is evident that the

increase in the chemical reaction (k_r) significantly alters the concentration boundary layer thickness but does not alter the momentum boundary layers.

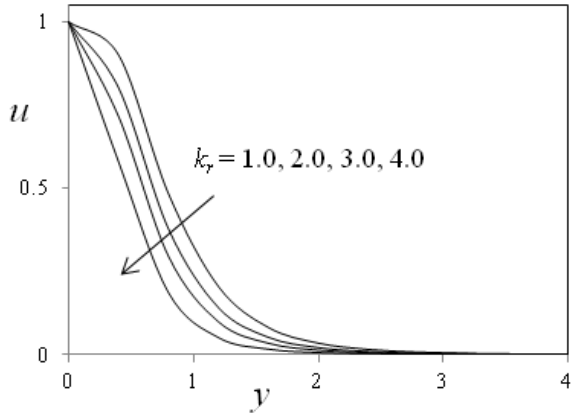

Figure 9. Velocity profiles for different values of k_r.

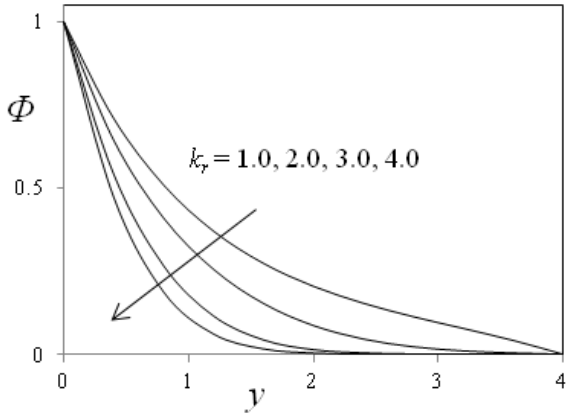

Figure 10. Concentration profiles for different values of k_r.

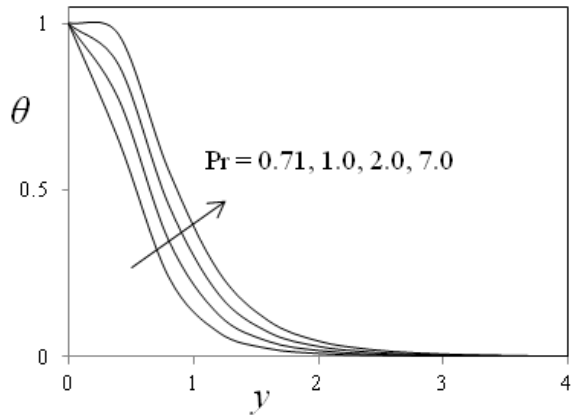

Figure 11. Temperature profiles for different values of Pr.

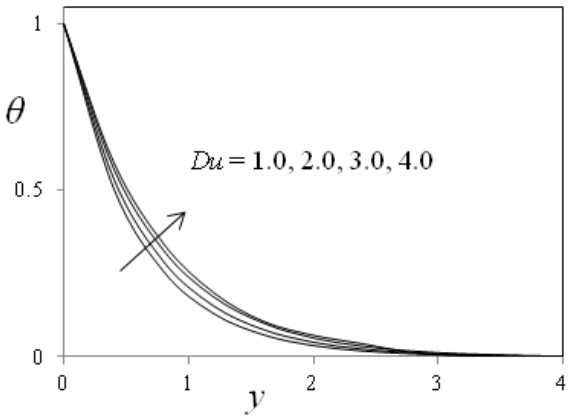

Figure 12. Temperature profiles for different values of *Du*.

In Fig. 11 we depict the effect of Prandtl number (Pr) on the temperature field. It is observed that an increase in the Prandtl number leads to decrease in the temperature field. Also, temperature field falls more rapidly for water in comparison to air and the temperature curve is exactly linear for mercury, which is more sensible towards change in temperature. From this observation it is conclude that mercury is most effective for maintaining temperature differences and can be used efficiently in the laboratory. Air can replace mercury, the effectiveness of maintaining temperature changes are much less than mercury. However, air can be better and cheap replacement for industrial purpose. This is because, either increase of kinematic viscosity or decrease of thermal conductivity leads to increase in the value of Prandtl number (Pr). Hence temperature decreases with increasing of Prandtl number (Pr). Fig. 12 depicts the effects of the Dufour number on the fluid temperature. It can be clearly seen from this figure that diffusion thermal effects slightly affect the fluid temperature. As the values of the Dufour number increase, the fluid temperature also increases.

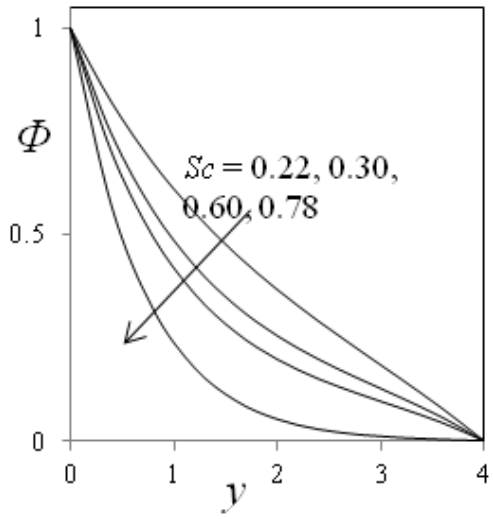

Figure 13. Concentration profiles for different values of Sc.

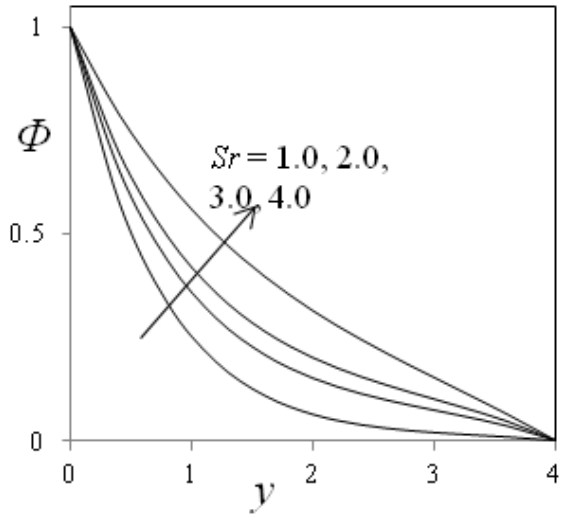

Figure 14. Concentration profiles for different values of Sr.

The effects of Schmidt number (Sc) and Soret number (Sr) on the concentration field are presented in Figs. 13-14. Fig. 13 shows the concentration field due to variation in Schmidt number (Sc) for the gasses Hydrogen, Helium, Water – vapour, Oxygen and Ammonia. It is observed that concentration field is steadily for Hydrogen and falls rapidly for Oxygen and Ammonia in comparison to Water – vapour. Thus Hydrogen can be used for maintaining effective concentration field and Water – vapour can be used for maintaining normal concentration field. In Fig. 14 it is observed that an increase in the Soret number (Sr) leads to increase in the concentration field.

Table 1. Skin – friction results for the values of *Gr, Gc, Pr, Sc, M, K, Ec, Sr, Du, R* and k_r.

Gr	*Gc*	*Pr*	*Sc*	*M*	*K*	*Ec*	*Sr*	*Du*	*R*	k_r	τ
1.0	1.0	0.71	0.22	1.0	1.0	0.001	1.0	1.0	1.0	1.0	5.74265944
2.0	1.0	0.71	0.22	1.0	1.0	0.001	1.0	1.0	1.0	1.0	5.91487712
1.0	2.0	0.71	0.22	1.0	1.0	0.001	1.0	1.0	1.0	1.0	6.02448526
1.0	1.0	7.00	0.22	1.0	1.0	0.001	1.0	1.0	1.0	1.0	5.55065597
1.0	1.0	0.71	0.30	1.0	1.0	0.001	1.0	1.0	1.0	1.0	5.56229532
1.0	1.0	0.71	0.22	2.0	1.0	0.001	1.0	1.0	1.0	1.0	5.61995047
1.0	1.0	0.71	0.22	1.0	2.0	0.001	1.0	1.0	1.0	1.0	5.81496621
1.0	1.0	0.71	0.22	1.0	1.0	0.100	1.0	1.0	1.0	1.0	5.76339115
1.0	1.0	0.71	0.22	1.0	1.0	0.001	2.0	1.0	1.0	1.0	5.78462910
1.0	1.0	0.71	0.22	1.0	1.0	0.001	1.0	2.0	1.0	1.0	5.79332183
1.0	1.0	0.71	0.22	1.0	1.0	0.001	1.0	1.0	2.0	1.0	5.88412656
1.0	1.0	0.71	0.22	1.0	1.0	0.001	1.0	1.0	1.0	2.0	5.66339541

The profiles for skin – friction (τ) due to velocity under the effects of Grashof number, Modified Grashof number, Prandtl number, Schmidt number, Hartmann number, Eckert number, Soret number, Dufour number, Thermal radiation parameter, Permeability parameter and Chemical reaction parameter are presented in the Table 1. We observe from Table 1 the skin – friction raises under the effects of Grashof number, Modified Grashof number, Eckert number, Soret number, Dufour number, Permeability parameter and Thermal radiation parameter. The skin – friction falls under the effects of Prandtl number, Schmidt number, Hartmann number and Chemical reaction parameter.

Table 2. Rate of heat transfer (*Nu*) values for different values of *Pr*, *Ec*, *R* and *Du*.

Pr	***Ec***	***Du***	***R***	***Nu***
0.71	0.001	1.0	1.0	5.12061452
7.00	0.001	1.0	1.0	5.06426925
0.71	0.100	1.0	1.0	5.18339674
0.71	0.001	2.0	1.0	5.22166705
0.71	0.001	1.0	2.0	5.23990477

The profiles for Nusselt number (Nu) due to temperature profile under the effect of Prandtl number, Eckert number, Thermal radiation parameter and Dufour number are presented in the Table 2. From this table we observe that, the Nusselt number due to temperature profile rises under the effect of Eckert number, Thermal radiation parameter and Dufour number. And temperature falls under the effect of Prandtl number.

Table 3. Rate of mass transfer (*Sh*) values for different values of *Sc*, *Sr* and k_r.

Sc	***Sr***	k_r	***Sh***
0.22	1.0	1.0	6.95461258
0.30	1.0	1.0	5.92215789
0.22	2.0	1.0	7.16023912
0.22	1.0	2.0	6.80418451

The profiles for Sherwood number (Sh) due to concentration profiles under the effect of Schmidt number, Soret number and Chemical reaction parameter are presented in the Table 3. We see from this table the Sherwood number due to concentration profile falls under the effect of Schmidt number and Chemical reaction parameter and rises under the effect of Soret number.

4. CONCLUSIONS

We summarize below the following results of physical interest on the velocity, temperature and concentration distributions of the flow field and also on the skin – friction, rate of heat and mass transfer at the wall.

– A growing Hartmann number or Chemical reaction parameter retards the velocity of the flow field at all points.

- The effect of increasing Permeability parameter or Eckert number or Permeability parameter or Soret number or Dufour number or Thermal radiation parameter are to accelerate velocity of the flow field at all points.
- A growing Prandtl number decreases temperature of the flow field at all points and increases with increasing of Eckert number or Dufour number or Thermal radiation parameter.
- The Schmidt number and Chemical reaction parameter decreases the concentration of the flow field at all points and increases with increasing of Soret number.
- A growing Hartmann number or Prandtl number or Schmidt number or Chemical reaction parameter decreases the skin – friction while increasing Grashof number or Modified Grashof number or Permeability parameter or Eckert number or Soret number or Dufour number or Thermal radiation parameter increases the skin – friction.
- The rate of heat transfer is decreasing with increasing of Prandtl number and increases with increasing of Eckert number, Thermal radiation parameter and Dufour number.
- The rate of mass transfer is decreasing with increasing of Schmidt number and Chemical reaction parameter and increasing with Soret number.

REFERENCES

[1] Ingham, D.B., Pop, I., *Transport phenomena in porous media III*, Elsevier, Oxford, 2005.
[2] Vafai, K., *Handbook of Porous media*, 2nd Ed., Taylor and Francis, New York, 2005.
[3] Kassoy, D.R., Zebib, A., *Physics of Fluids*, **18**, 1649, 1975.
[4] Cheng, P., Minkowycz, W.J., *J. Geophys. Res*., **82**, 2040, 1977.
[5] Bejan, A., Khair, K.R., *International Journal of Heat Mass Transfer*, **28**(5), 909, 1985.
[6] Lai, F.C., Kulacki, F.A., *International Journal of Heat Mass Transfer*, **33**, 1028, 1990.
[7] Lai, F.C., Kulacki, F.A., *International Journal of Heat Mass Transfer*, **34**(4/5), 1189, 1991.
[8] Yih, K.A., *Int. Comm. Heat Mass Transfer*, **25**(8), 1145, 1998.
[9] Kumari, M., *Mech. Res. Commun*., **28**, 339, 2001.
[10] Postelnicu, A., Grosan, T., Pop, I., *Mech. Res. Commun*., **28**, 331, 2001.
[11] Seddeek, M.A., *Acta Mech*., **177**, 1, 2005.
[12] Seddeek, M.A., Salem, A.M., *Int. J. Heat and Mass Transfer*, **41**, 1048, 2005.
[13] Mohamed, E.A., *Int. J. of Thermal Sciences*, **45**, 60, 2006.
[14] Alam, M.S., Rahman, M.M., Samad, M.A., *Non – linear Analysis Modeling and Control*, **11**(4), 331, 2006.
[15] Pantokratoras, A., *Int. J. of Thermal Sciences*, **45**, 378, 2006.
[16] Ramana Reddy, G.V., Ramana Murthy, C.V., Bhaskar Reddy, N., *Mathematics Applied in Science and Technology*, **1**(1), 65, 2009.
[17] Sparrow, E.M., Cess, R.D., *Int J Heat Mass Transfer*., **3**, 267, 1961.
[18] Alam, M.S., Rahman, M.M., *Journal of Noval Architecture and Marine Engineering*, **2**(1), 55, 2005.
[19] Dursunkaya, Z., Worek, W.M., *International Journal of Heat and Mass Transfer*, **35**(8), 2060, 1992.

[20] Postelnicu, A., *International Journal of Heat and Mass Transfer*, **47**(67), 1467, 2004.
[21] Raptis, A., Perdikis, C., *Appl. Mech. Eng.*, **4**(4), 817, 1999.
[22] Satyanarayana, P.V., Kesavaiah, D.C., Venkataramana, S., *International Journal of Mathematical Archive*, **2**(4), 476, 2011.
[23] Alabraba, M.A., Bestman, A.R., Ogulu, A., *Astrophysics and Space Science*, **195**(2), 431, 1992.
[24] Enamul Karim, M.D., Abdus Samad, M.D., Maruf Hasan, M.D., *Open Journal of Fluid Dynamics*, **2**, 91, 2012.
[25] Bhavana, M., Kesaraiah Chenna, D., Sudhakarraiah, A., *Int. J. of Innovative R. in Sci. Eng. and Tech*., **2**(5), 1617, 2013.
[26] Brewster, M.Q., *Thermal radiative transfer & properties*, John Wiley & Sons, 1992.